An International Journal of Optimization and Control: Theories & Applications
ISSN:2146-0957 eISSN:2146-5703
Vol.9, No.2, pp.223-235 (2019)
http://doi.org/10.11121/ijocta.01.2019.00709

RESEARCH ARTICLE

A mixed method approach to Schrödinger equation: Finite difference method and quartic B-spline based differential quadrature method

Ali Başhan[a]

Department of Mathematics, University of Zonguldak Bulent Ecevit, Turkey
alibashan@gmail.com

ARTICLE INFO

Article History:
Received 12 September 2018
Accepted 16 May 2019
*Available ** July 2019*

Keywords:
Differential quadrature method
Finite difference method
Quartic B-Splines
Nonlinear Schrödinger equation

AMS Classification 2010:
65M99; 65D07; 15A30

ABSTRACT

The present manuscript includes finite difference method and quartic B-spline based differential quadrature method (FDM-DQM) for getting the numerical solutions for the nonlinear Schrödinger (NLS) equation. To solve complex NLS equation firstly we have separated NLS equation into the two real value partial differential equations. After that they are discretized in time using special type of classical finite difference method namely, Crank-Nicolson scheme. Then, for space integration differential quadrature method has been implemented. So, partial differential equation turn into simple a system of algebraic equations. To display the accuracy of the present hybrid method, the error norms L_2 and L_∞ and two lowest invariants I_1 and I_2 and relative changes of invariants have been calculated. As a last step, the numerical result already obtained have been compared with earlier studies by using same parameters. The comparison has clearly indicated that the presently used method, namely FDM-DQM, is an appropriate and accurate numerical scheme and allowed us to present for solving a wide class of partial differential equations.

1. Introduction

In recent years, studies on findings numerical solutions of differential equations have took attention of researchers throughout over the world [1–6]. In nature, several physical phenomena can easily be defined by NLS equation such as propagation of optical pulses, waves in water, waves in plasmas, and self focusing in laser pulses. Because of this, among others, several authors have tried hard to present analytical solutions of NLS [7–9] and numerical solutions have been studied [10–18]. NLS equation has a nature of attracting the attention of a lot of researchers for illustrate the efficiency of the numerical methods. Therefore, recently, many studies of different methods such as quadratic FEM [19], radial based collocation method [20], Taylor collocation method based on cubic B-spline [21], quintic B-spline based FEM [22] for the NLS equation may be encountered.

Firstly, we will handle the NLS equation given in the following form

$$iz_t + z_{xx} + \gamma |z|^2 z = 0 \quad a \le x \le b, \quad t \in [0, T] \tag{1}$$

together having the boundary conditions

$$z(a,t) = z(b,t) = 0$$

where $i = \sqrt{-1}$, γ is a real parameter. Meanwhile the subscripts t and x describe partial derivatives with respect to time and space, respectively.

For being capable of computing the complex function z, we have to separate it into the two real value functions by rewriting

$$z(x,t) = u(x,t) + iv(x,t), \tag{2}$$

in which both $u(x,t)$ and $v(x,t)$ are real functions. Upon substituting (2) into the Eq.(1) it results in coupled real value partial differential equation system

$$\begin{aligned} u_t + v_{xx} + \gamma\left[u^2 v + v^3\right] &= 0, \\ v_t - u_{xx} - \gamma\left[v^2 u + u^3\right] &= 0. \end{aligned} \quad (3)$$

After applying the boundary conditions to (2) newly obtained boundary conditions may be stated in the following form

$$\begin{aligned} u(a,t) &= u(b,t) = 0, \\ v(a,t) &= v(b,t) = 0. \end{aligned} \quad (4)$$

DQM, first introduced by Bellman *et al.* [24] in 1972, has had wide application areas due to its considerably less number of mesh points usage. When one search the literature, it can be seen that many scientists have improved different types of DQM using various base functions [24–35]. In this study, fourth order quartic B-spline based FDM-DQM will be used to obtain numerical solutions of the NLS equation.

2. Fourth order quartic B-spline based DQM

Let us take the grid distribution $a = x_1 < x_2 < \cdots < x_N = b$ of a finite interval $[a,b]$ into consideration. Under the condition that a function $U(x)$ is enough smooth over the solution domain, its derivatives with respect to x at a grid point x_i can be approximated by a linear combination of all the functional values over the solution domain of the problem, that is,

$$\begin{aligned} \frac{d^{(r)}U}{dx^{(r)}} \quad | \quad_{x_i} &= \sum_{j=1}^{N} w_{ij}^{(r)} U(x_j), \quad (5) \\ i &= 1,2,...,N, \quad r = 1,2,...,N-1 \end{aligned}$$

where r represents the order of the derivative, $w_{ij}^{(r)}$ denote the weighting coefficients of the r^{th} order derivative approximation and N denotes the number of mesh points in the solution domain. Here, the index j emphasizes the fact that $w_{ij}^{(r)}$ is the corresponding weighting coefficient of the functional value $U(x_j)$.

In this study, we need the first order and the second order derivative of the function $U(x)$. So, firstly we will find value of the equation (5) for the $r = 1$.

Let $Q_s(x)$, be the quartic B-splines having nodes at the points x_i where the uniformly distributed N nodal points are taken into consideration as $a = x_1 < x_2 < \cdots < x_N = b$ on the ordinary real axis. Then, the B-splines $\{Q_{-1}, Q_0, \ldots, Q_{N+1}\}$ constitute a basis for functions defined over $[a,b]$. The quartic B-splines $Q_s(x)$ are described by the relationships:

$$Q_s(x) = \frac{1}{h^4}\begin{cases} q_1, & x \in [x_{s-2}, x_{s-1}], \\ q_1 - 5q_2, & x \in [x_{s-1}, x_s], \\ q_1 - 5q_2 + 10q_3, & x \in [x_s, x_{s+1}], \\ q_4 - 5q_5, & x \in [x_{s+1}, x_{s+2}], \\ q_4, & x \in [x_{s+2}, x_{s+3}], \\ 0, & otherwise. \end{cases}$$

where $q_1 = (x - x_{s-2})^4$, $q_2 = (x - x_{s-1})^4$, $q_3 = (x - x_s)^4$, $q_4 = (x_{s+3} - x)^4$ $q_5 = (x_{s+2} - x)^4$, $h = x_s - x_{s-1}$ for all s.

Table 1. Quartic B-splines and their corresponding derivatives at the nodal points.

x	x_{s-2}	x_{s-1}	x_s	x_{s+1}	x_{s+2}	x_{s+3}
Q	0	1	11	11	1	0
hQ'	0	4	12	-12	-4	0
h$^2Q''$	0	12	-12	-12	12	0
h$^3Q'''$	0	24	-72	72	-24	0

Using the quartic B-splines as trial functions in the fundamental DQM equation (5) results in to the equation

$$\begin{aligned} \frac{d^{(r)}Q_s(x_i)}{dx^{(r)}} &= \sum_{j=s-1}^{s+2} w_{i,j}^{(r)} Q_s(x_j), \quad (6) \\ s &= -1, 0, \ldots, N+1, \; i = 1,2,...,N. \end{aligned}$$

2.1. *The 1^st order weighting coefficients*

When DQM methodology is applied, the fundamental equality for determining the corresponding weighting coefficients of the first order derivative approximation is obtained as Korkmaz used [29]:

$$\begin{aligned} \frac{dQ_s(x_i)}{dx} &= \sum_{j=s-1}^{s+2} w_{i,j}^{(1)} Q_s(x_j), \quad (7) \\ s &= -1, 0, \ldots, N+1, \; i = 1,2,...,N. \end{aligned}$$

In the process, the initial step for finding out the corresponding weighting coefficients $w_{i,j}^{(1)}$, $j = -2, -1, \ldots, N+3$ of the first grid point x_1 is to apply the test functions Q_s, $s = -1, 0, \ldots, N+1$ at the grid point x_1. After all the Q_s trial functions are applied, we obtain the following algebraic equation system:

$$A_1.\begin{bmatrix} w_{1,-2}^{(1)} \\ w_{1,-1}^{(1)} \\ w_{1,0}^{(1)} \\ w_{1,1}^{(1)} \\ w_{1,2}^{(1)} \\ \vdots \\ w_{1,N+2}^{(1)} \\ w_{1,N+3}^{(1)} \end{bmatrix} = \begin{bmatrix} -\frac{4}{h} \\ -\frac{12}{h} \\ \frac{12}{h} \\ \frac{4}{h} \\ 0 \\ \vdots \\ 0 \\ 0 \end{bmatrix} \tag{8}$$

where

$$A_1 = \begin{bmatrix} 1 & 11 & 11 & 1 & & & & \\ & 1 & 11 & 11 & 1 & & & \\ & & \ddots & \ddots & \ddots & \ddots & & \\ & & & & & & & \\ & & & 1 & 11 & 11 & 1 & \\ & & & & 1 & 11 & 11 & 1 \end{bmatrix}$$

The weighting coefficients $w_{1,j}^{(1)}$ related to the first grid point are determined by solving equation system (8). The equation system (8) composed of $N+6$ unknowns and $N+3$ equations. To have a distinct solution, it is required to add three additional equations to the system. By the derivations of the equations

$$\frac{d^2 Q_{-1}(x_1)}{dx^2} = \sum_{j=-2}^{1} w_{1,j}^{(1)} Q'_{-1}(x_j) \tag{9}$$

$$\frac{d^2 Q_{N}(x_1)}{dx^2} = \sum_{j=N-1}^{N+2} w_{1,j}^{(1)} Q'_{N}(x_j) \tag{10}$$

$$\frac{d^2 Q_{N+1}(x_1)}{dx^2} = \sum_{j=N}^{N+3} w_{1,j}^{(1)} Q'_{N+1}(x_j) \tag{11}$$

is obtained. By using the equations (9), (10) and (11) which we obtained by derivations, three unknown terms will be eliminate from equation system.

$$A_2.\begin{bmatrix} w_{1,-1}^{(1)} \\ w_{1,0}^{(1)} \\ w_{1,1}^{(1)} \\ w_{1,2}^{(1)} \\ w_{1,3}^{(1)} \\ \vdots \\ w_{1,N}^{(1)} \\ w_{1,N+1}^{(1)} \end{bmatrix} = \begin{bmatrix} -\frac{7}{h} \\ -\frac{12}{h} \\ \frac{12}{h} \\ \frac{4}{h} \\ 0 \\ \vdots \\ 0 \\ 0 \end{bmatrix} \tag{12}$$

where

$$A_2 = \begin{bmatrix} 8 & 14 & 2 & & & & \\ 1 & 11 & 11 & 1 & & & \\ & \ddots & \ddots & \ddots & \ddots & & \\ & & & & & & \\ & & & 1 & 11 & 11 & 1 \\ & & & & 2 & 14 & 8 \\ & & & & & 30 & 42 \end{bmatrix}$$

So, the number of algebraic equations and the unknowns will be equal and the equation system will be solved with Thomas algorithm. The new matrix system(12) contains $N+3$ equations and $N+3$ unknowns. By the same idea, for the determine weighting coefficients $w_{k,j}^{(1)}$, $j=-1,0,\dots,N+1$ at grid points x_k, $2 \le k \le N-1$ we got the algebraic equation system:

$$A_2.\begin{bmatrix} w_{k,-1}^{(1)} \\ \vdots \\ w_{k,k-3}^{(1)} \\ w_{k,k-2}^{(1)} \\ w_{k,k-1}^{(1)} \\ w_{k,k}^{(1)} \\ w_{k,k+1}^{(1)} \\ w_{k,k+2}^{(1)} \\ \vdots \\ w_{k,N+1}^{(1)} \end{bmatrix} = \begin{bmatrix} 0 \\ \vdots \\ 0 \\ \frac{-4}{h} \\ \frac{-12}{h} \\ \frac{12}{h} \\ \frac{4}{h} \\ 0 \\ \vdots \\ 0 \end{bmatrix} \tag{13}$$

For the last grid point of the domain x_N with same idea, determine weighting coefficients $w_{N,j}^{(1)}$, $j=-1,0,\dots,N+1$ we got the algebraic equation system:

$$A_2.\begin{bmatrix} w_{N,-1}^{(1)} \\ w_{N,0}^{(1)} \\ \vdots \\ w_{N,N-3}^{(1)} \\ w_{N,N-2}^{(1)} \\ w_{N,N-1}^{(1)} \\ w_{N,N}^{(1)} \\ w_{N,N+1}^{(1)} \end{bmatrix} = \begin{bmatrix} 0 \\ 0 \\ \vdots \\ 0 \\ \frac{-4}{h} \\ \frac{-12}{h} \\ \frac{9}{h} \\ \frac{53}{h} \end{bmatrix} \tag{14}$$

2.2. *The 2^{nd}* **order** *weighting coefficients*

If we use matrix multiplication approach, then all the corresponding weighting coefficients can be found out. The present method is based on the first order weighting coefficients to obtain the weighting coefficients of the second order derivatives. When one uses matrix multiplication procedure, the second order weighting coefficients are determined as below [23]:

$$\left[A^{(2)}\right]=\left[A^{(1)}\right]\left[A^{(1)}\right], \quad (15)$$

where $\left[A^{(1)}\right], \left[A^{(2)}\right]$ are the weighting coefficients matrices of the first- and the second-order derivatives, respectively [23].

3. Discretization of the mixed method

The Eq. system (3) is given of the form

$$\begin{aligned} u_t+v_{xx}+\gamma\left[u^2v+v^3\right] &= 0, \quad (16)\\ v_t-u_{xx}-\gamma\left[v^2u+u^3\right] &= 0. \quad (17)\end{aligned}$$

One can implement Crank-Nicolson scheme to Eq. (16) and easily obtain

$$\begin{aligned} &\frac{u^{n+1}-u^n}{\Delta t}+\frac{v_{xx}^{n+1}+v_{xx}^n}{2}+\\ &\gamma\left[\frac{\left(v^3\right)^{n+1}+\left(v^3\right)^n}{2}\right]+\\ &\gamma\left[\frac{\left(u^2v\right)^{n+1}+\left(u^2v\right)^n}{2}\right]\\ =\ &0. \quad (18)\end{aligned}$$

After that, the rearrangement of Eq. (18) yields the following form

$$\begin{aligned} &2u^{n+1}+\Delta t\left[v_{xx}^{n+1}+\gamma\left(\left(v^3\right)^{n+1}+\left(u^2v\right)^{n+1}\right)\right]\\ =\ &2u^n-\Delta t\left[v_{xx}^n+\gamma\left(\left(v^3\right)^n+\left(u^2v\right)^n\right)\right]. \quad (19)\end{aligned}$$

If we use the Rubin and Graves linearization techniques [36] in Eq. (19) to vanish the nonlinear terms, thus one obtains the linear equation

$$\begin{aligned} &2u^{n+1}+\Delta t\left[\begin{array}{c} v_{xx}^{n+1}+3\gamma\left(v^2\right)^n v^{n+1}+\\ \gamma\left(u^2\right)^n v^{n+1}+2\gamma u^n v^n u^{n+1}\end{array}\right]\\ =\ &2u^n+\Delta t\left[-v_{xx}^n+\gamma\left(v^3\right)^n+\gamma\left(u^2v\right)^n\right]. \quad (20)\end{aligned}$$

Some simple organizations for Eq. (20) and definitions as stated below are made

$$\begin{aligned} A_i^n &= \sum_{j=1}^N w_{i,j}^{(2)}U_j^n=U_{xx_i}^n,\\ B_i^n &= \sum_{j=1}^N w_{i,j}^{(2)}V_j^n=V_{xx_i}^n,\\ U_{xx_i}^{n+1} &= \sum_{j=1}^N w_{i,j}^{(2)}U_j^{n+1},\ V_{xx_i}^{n+1}=\sum_{j=1}^N w_{i,j}^{(2)}V_j^{n+1}\\ \Phi_i^n &= 2U_i^n+ \quad (21)\\ &\quad \Delta t\left[-B_i^n+\gamma\left(V_i^n\right)^3+\gamma\left(U_i^n\right)^2V_i^n\right]\\ \Psi_i^n &= 2V_i^n+\\ &\quad \Delta t\left[A_i^n-\gamma\left(U_i^n\right)^3-\gamma\left(V_i^n\right)^2U_i^n\right]\end{aligned}$$

for $i=1(1)N$. When substituted Eq. (21) into Eq. (20) one can obtain

$$\begin{aligned} &2U_i^{n+1}+\\ &\Delta t\left[\begin{array}{c}\sum_{j=1}^N w_{i,j}^{(2)}V_j^{n+1}+\\ \gamma\left(\begin{array}{c}3\left(V_i^n\right)^2V_i^{n+1}+\\ \left(U_i^n\right)^2V_i^{n+1}+2U_i^nV_i^nU_i^{n+1}\end{array}\right)\end{array}\right]\\ =\ &\Phi_i^n. \quad (22)\end{aligned}$$

When we make some arrangements in Eq. (22), we obtain the following equation

$$\begin{aligned} &\left[2+2\gamma\Delta tU_i^nV_i^n\right]U_i^{n+1}+\\ &\left[\Delta t\left(w_{i,i}^{(2)}+\gamma\left(3\left(V_i^n\right)^2+\left(U_i^n\right)^2\right)\right)\right]V_i^{n+1}\\ &+\sum_{j=1,i\neq j}^N\left(\Delta tw_{i,j}^{(2)}\right)V_j^{n+1}\\ =\ &\Phi_i^n\ . \quad (23)\end{aligned}$$

Using the same procedure the same process now for Eq. (17), the following equation is obtained

$$\begin{aligned} &\left[-\Delta t\left(w_{i,i}^{(2)}+\gamma\left(3\left(U_i^n\right)^2+\left(V_i^n\right)^2\right)\right)\right]U_i^{n+1}\\ &+\sum_{j=1,i\neq j}^N\left(-\Delta tw_{i,j}^{(2)}\right)U_j^{n+1}+\\ &\left[2-2\gamma\Delta tU_i^nV_i^n\right]V_i^{n+1}\\ =\ &\Psi_i^n\ . \quad (24)\end{aligned}$$

When the boundary conditions in Eq. (4), are used the algebraic equation system in the form of $(2N-4)\times(2N-4)$ matrix is obtained and solved by Gauss elimination.

4. Numerical studies

In this part, four famous problems namely single soliton, double solitons, standing soliton and mobile soliton have been searched. The efficiency of the proposed newly scheme is checked using the two error norms L_2 and L_∞, respectively:

$$\begin{aligned} L_2 &= \|u-U\|_2 \simeq \sqrt{h\sum_{j=1}^{N}\left|u_j^{exact}-(U_N)_j\right|^2}, \\ L_\infty &= \|u-U\|_\infty \simeq \max_j \left|u_j^{exact}-(U_N)_j\right|, \\ j &= 1\,(1)\,N. \end{aligned}$$

Besides error norms L_2 and L_∞, the lowest two invariants, of which formulae are presented below, are computed

$$\begin{aligned} I_1 &= \int_a^b |u|^2 dx \\ &\approx h\sum_{j=0}^{N}\left|U_j^n\right|^2, \\ I_2 &= \int_a^b \left[|u_x|^2 - \tfrac{\gamma}{2}|u|^4\right] dx \\ &\approx h\sum_{j=0}^{N}\left[|\,(U_x)_j^n\,|^2 - \tfrac{\gamma}{2}|U_j^n|^4\right]. \end{aligned}$$

Relative changes of invariants described by $\widehat{I}_j = \frac{I_j^{final}-I_j^{initial}}{I_j^{initial}}$, $j=1,2$ have been checked.

4.1. Single Soliton

The first example has been taken into consideration as the motion of single soliton of which exact solution is presented of the form

$$\begin{aligned} z(x,t) &= \alpha\sqrt{\frac{2}{\gamma}}. \\ &\exp i\left\{\frac{2\sigma x - \left(\sigma^2-\alpha^2\right)t}{4}\right\}. \\ &\operatorname{sech}\,\alpha\,(x-\sigma t) \end{aligned} \tag{25}$$

where σ represents the velocity of the single soliton of which amplitude depends on α. We have selected the values of $\gamma=2, \sigma=4, \alpha=1$ and $\alpha=2$ at the solution domain $-20 \le x \le 20$ just capable of comparing with earlier studies. When $\alpha=1$ is taken the envelop soliton

$$|z| = \operatorname{sech}\ (x-4t)$$

moves toward the right with unchanged characteristics such as speed $\sigma=4$, shape, and amplitude $\alpha=1$. For visual representation, the simulations of single soliton for values of $\Delta t=0.005$, $N=291$at various times from $t=0$ to $t=4$ are plotted in Figure 1. As it is seen obviously from Figure 1, the real and imaginary parts of the z separately and the module $|z|$ is given.

To compare the results, the values of the error norms L_2 and L_∞, and the two lowest invariants I_1 and I_2, and relative changes of invariants are illustrated in comparison with quadratic B-spline based finite element method [19] for values of $\Delta t=0.005$ and $N=291$ at several times in Table 2. As one can see clearly from Table 2, by using the same parameters and less number of the nodal points than earlier work [19] the new results are better than quadratic B-spline based finite element method [19] solutions.

A deeper comparison of numerical results, for amplitude $\alpha=1$, at time $t=1$ is given in Table 3. It can be obviously seen from Table 3 that by decreasing the time increments, the error norm L_∞ of FDM-DQM get decreased to the 1.5×10^{-4}. Those are the best results in the presented results.

One can see the comparison of numerical results with another studies that Gaussian, Multiquadric, Inverse Multiquadric and Inverse Quadric radial based collocation method [20] , for amplitude $\alpha=1$, at time $t=2.5$ in Table 4. The error norms L_2 and L_∞ of FDM-DQM are the best results among all given results except the Gaussian radial based collocation method.

Similar to the solutions of amplitude $\alpha=1$, for the bigger amplitude $\alpha=2$, results have been illustrated with comparison of earlier studies at time $t=1$ at Table 5. One more time, by decreasing the time steps the error norm L_∞ of FDM-DQM decrease to the 2.5×10^{-4} which is the best result for NLS equation in the all given studies.

4.2. Double solitons

In our second trial example, the initial condition of collision of double solitons is taken as follows [10]:

$$z(x,0) = \sum_{k=1}^{2} z_k(x,0) \tag{26}$$

where

$$\begin{aligned} z_k(x,0) &= \alpha_k\sqrt{\frac{2}{\gamma}}. \\ &\exp i\left\{\frac{\sigma_k}{2}(x-x_k)\right\}. \\ &\operatorname{sech}\,\alpha_k\,(x-x_k), \\ k &= 1,2. \end{aligned} \tag{27}$$

We have chosen the values of $\gamma=2$, $\alpha_1=\alpha_2=1$, $\sigma_1=-4$, $\sigma_2=4$, $x_1=10$, and $x_2=-10$ over the region $-20 \le x \le 20$. These simulations show the

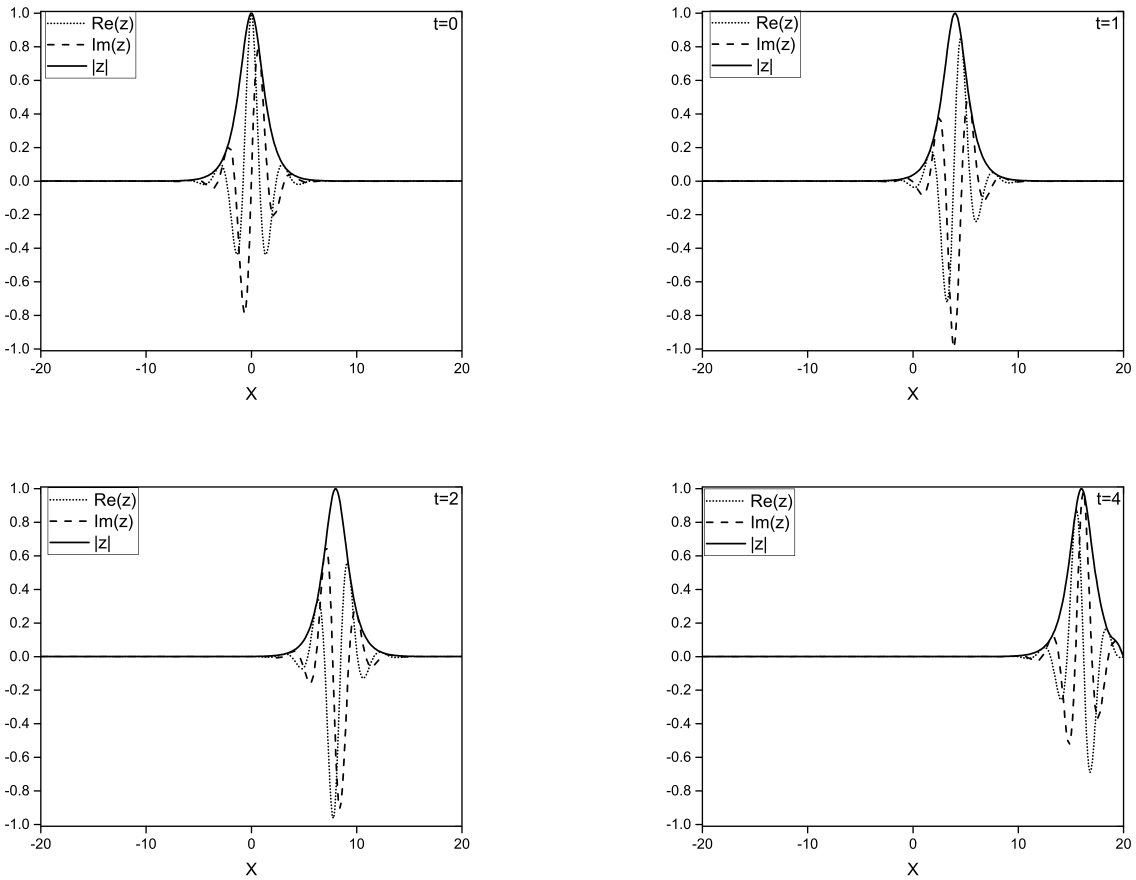

Figure 1. Simulation of single soliton $\Delta t = 0.005, N = 291$.

Table 2. Error norms, invariants and relative changes of invariants: $\Delta t = 0.005$.

	Present (FDM-DQM) N=291						Quad. FEM [19] N=800			
t	I_1	I_2	$\widehat{I_1}$	$\widehat{I_2}$	L_2	L_∞	I_1	I_2	L_2	L_∞
0.0	2.00000	7.33370	-	-	0.00000	0.00000	2.0	7.3537736	0.0000	0.0000
0.5	2.00000	7.33371	1.0×10^{-6}	8.2×10^{-7}	0.00012	0.00008	2.0	7.3537756	0.0002	0.0002
1.0	2.00001	7.33373	4.0×10^{-6}	3.7×10^{-6}	0.00023	0.00015	2.0	7.3537778	0.0004	0.0003
1.5	2.00001	7.33374	5.5×10^{-6}	4.4×10^{-6}	0.00032	0.00021	2.0	7.3537793	0.0007	0.0004
2.0	2.00001	7.33375	6.0×10^{-6}	6.1×10^{-6}	0.00040	0.00026	2.0	7.3537802	0.0008	0.0005
2.5	2.00001	7.33377	6.5×10^{-6}	9.4×10^{-6}	0.00047	0.00029	2.0	7.3537803	0.0009	0.0006

collision of two solitons at the different positions which are $x_1 = 10$, and $x_2 = -10$ in the opposite ways with same amplitudes, $\alpha_1 = \alpha_2 = 1$, and same speeds, $\sigma_1 = \sigma_2 = 4$. Due to characteristics of solitons, after the collision finished double solitons conserve their properties such as shape, speed and amplitudes, which can be seen at the simulations of double solitons shown in Figure 2. The simulations are run up to the time $t = 5.5$. As time increases, collision begins close to $t = 2$ and height of the amplitudes nearly $\alpha = 2$ observed at time $t = 2.5$. At the time interaction ends at time $t = 5.5$, two solitons preserve their originally properties like the initial position.

Two lowest invariants of the this method is presented with comparison of earlier works, in Table 6. Particularly at interaction typical observed at time $t = 2.5$ changes of two invariants I_1 and I_2 have more importance for efficiency of the implemented methods. As it is seen in Table 6 that relative changes of the invariants I_1 and I_2 at collision time $t = 2.5$ are -1.0×10^{-6} and -3.4×10^{-6}, respectively and in the end of the simulations this changes are 2.5×10^{-7} and -6.8×10^{-7}, respectively.

The obtained new results are presented and compared with earlier studies in Table 6. Numerical results are clearly shows that more particularly at

Table 3. L_∞ error norm and relative changes of invariants of single soliton: $amp. = 1, t = 1$.

Method	N	h	Δt	L_∞	$\widehat{I_1}$	$\widehat{I_2}$
FDM-DQM	152	0.26	0.02	0.00254	1.9×10^{-4}	2.2×10^{-4}
(Present)	291	0.14	0.005	0.00015	4.0×10^{-6}	3.7×10^{-6}
Quad.Gal. [19]		0.3125	0.02	0.002	0.0000066	-0.0003417
		0.05	0.005	0.0003	0.0000000	0.0000006
Quin. Coll. [22]		0.3125	0.02	0.002	0.0000000	0.0000063
		0.05	0.005	0.0003	0.0000000	0.0000000
Tay.Coll. [21]		0.3125	0.02	0.00176	0.0000019	0.000016
		0.05	0.005	0.00026	-0.00000002	-0.00000003
Cub. Coll. [15]		0.05	0.005	0.008	0.00000	0.00000
		0.03	0.005	0.002	0.00000	0.00000
Explicit [11]		0.05	0.000625	0.00564	0.00000	-0.00556
Implicit/Explicit [11]		0.05	0.001	0.00577	-0.00393	-0.01205
Implicit Cr-Ni. [11]		0.05	0.005	0.00585	-0.00001	-0.00557
Hopscotch [11]		0.08	0.002	0.00538	0.00003	-0.01407
Split step Four. [11]		0.3125	0.02	0.00466	0.00000	0.00005
A-L Local [11]		0.06	0.0165	0.00580	0.00004	-0.00797
A-L Global [11]		0.05	0.04	0.00561	0.00003	0.00550
Pseudospectral [11]		0.3125	0.0026	0.00513	0.00001	-0.00003

Table 4. L_2 and L_∞ error norms and invariants of single soliton: $amp. = 1, t = 2.5$.

Method	N	h	Δt	L_2	L_∞	I_1	I_2
FDM-DQM	291	0.14	0.005	0.000226	0.000153	2.000008	7.333730
G [20]		0.3125	0.001	0.000046	0.000028	1.999908	7.333177
MQ [20]		0.3125	0.001	0.004434	0.002165	1.999472	7.331960
IMQ [20]		0.3125	0.001	0.000668	0.000486	1.999137	7.329795
IQ [20]		0.3125	0.001	0.005652	0.002037	1.999812	7.329801

Table 5. L_∞ error norm and relative changes of invariants of single soliton, $amp. = 2, t = 1$.

Method	N	h	Δt	L_∞	$\widehat{I_1}$	$\widehat{I_2}$
FDM-DQM	386	0.1	0.005	0.00031	0.0×10^{-13}	4.5×10^{-5}
(Present)	391	0.1	0.0048	0.00028	-5.0×10^{-7}	3.8×10^{-5}
	491	0.08	0.0025	0.00025	-2.5×10^{-6}	1.4×10^{-5}
Quad.Gal. [19]		0.1	0.005	0.0004	0.00000001	-0.000008
		0.1563	0.0048	0.004	0.0000095	-0.000276
Quin. Coll. [22]		0.015	0.005	0.001	0.0000000	0.0000001
		0.1	0.005	0.0007	0.0000000	0.0000000
		0.1563	0.0048	0.002	0.0000000	0.0000026
		0.02	0.0025	0.0003	0.0000000	0.0000000
Tay.Coll. [21]		0.05	0.005	0.00104	0.00000002	-0.00000017
		0.1	0.005	0.00076	0.00000006	0.00000003
		0.1563	0.0048	0.00207	0.00000034	0.00000358
Cub. Coll. [15]		0.015	0.005	0.008	0.00000	0.00025
		0.02	0.0025	0.011	0.00000	0.00004
Explicit [11]		0.02	0.0001	0.00931	-0.00437	-0.00284
Implicit/Explicit [11]		0.03	0.00022	0.00759	0.00003	-0.02243
Implicit Cr-Ni. [11]		0.02	0.011	0.00971	0.00000	-0.00273
Hopscotch [11]		0.02	0.0004	0.00963	0.00002	-0.00284
Split step Four. [11]		0.1563	0.0048	0.00464	0.00000	0.00034
A-L Local [11]		0.06	0.03	0.00695	-0.00001	-0.02526
A-L Global [11]		0.07	0.012	0.00937	-0.00004	-0.03324
Pseudospectral [11]		0.1563	0.0011	0.00840	0.00000	0.00005

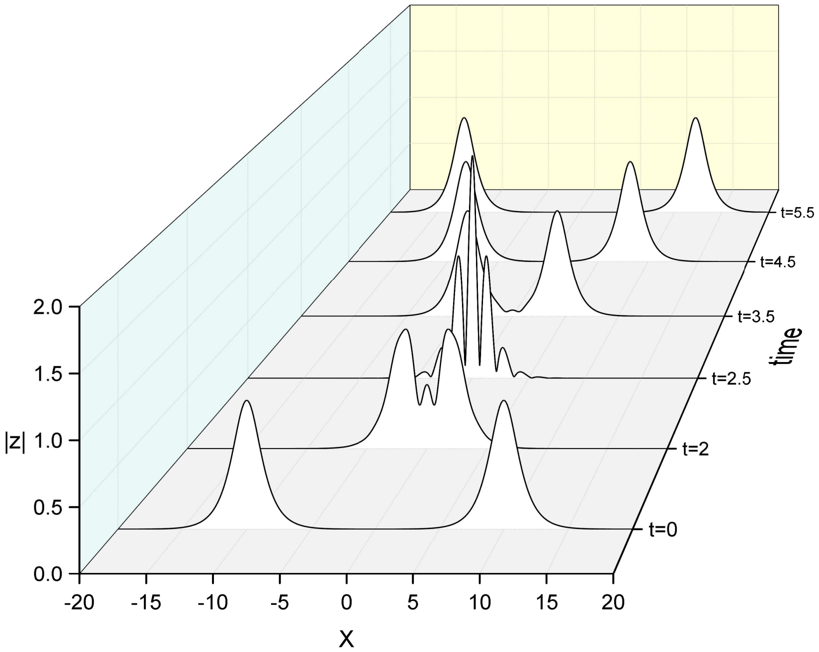

Figure 2. Double solitons $\alpha_1 = \alpha_2 = 1$.

Table 6. Invariants and relative changes of invariants of double solitons:$\alpha_1 = \alpha_2 = 1$

	Present (FDM-DQM)				Cub. Coll. [15]		Quad.Gal. [19]	
t	I_1	I_2	$\widehat{I}_1$	$\widehat{I}_2$	I_1	I_2	I_1	I_2
0.0	3.999998	14.66677	-	-	3.99998	14.66596	3.99999	14.83143
0.5	3.999996	14.66668	-5.0×10^{-7}	-6.1×10^{-6}	3.99998	14.66644	3.99999	14.83150
1.0	3.999999	14.66668	2.5×10^{-7}	-6.1×10^{-6}	3.99998	14.66706	3.99999	14.83157
1.5	4.000000	14.66667	5.0×10^{-7}	-6.8×10^{-6}	3.99999	14.66753	3.99999	14.83161
2.0	3.999998	14.66668	0.0×10^{-13}	-6.1×10^{-6}	3.99999	14.66693	3.99999	14.83261
2.5	3.999994	14.66672	-1.0×10^{-6}	-3.4×10^{-6}	3.99998	14.61440	3.99999	14.95380
3.0	3.999998	14.66667	0.0×10^{-13}	-6.8×10^{-6}	3.99998	14.66789	3.99999	-
3.5	3.999999	14.66668	2.5×10^{-7}	-6.1×10^{-6}	3.99999	14.66781	3.99999	14.83161
4.0	3.999996	14.66668	-5.0×10^{-7}	-6.1×10^{-6}	3.99998	14.66746	3.99999	14.83158
4.5	3.999997	14.66669	0.0×10^{-13}	-5.5×10^{-6}	3.99999	14.66613	3.99999	14.83156
5.0	3.999997	14.66667	-2.5×10^{-7}	-6.8×10^{-6}	3.99999	14.66684	3.99999	14.83153
5.5	3.999999	14.66676	2.5×10^{-7}	-6.8×10^{-7}	3.99999	14.66669	4.00000	14.83153

the critical time of collision $t = 2.5$ FDM-DQM solutions are better than cubic B-spline based FEM [15] and quadratic B-spline based FEM [19].

4.3. The standing soliton

Our next problem, having an initial condition $z(x, 0)$, a soliton is taken. The theory says that if

$$I = \int_{-\infty}^{\infty} z(x, 0)dx \geq \pi$$

then a soliton will appear with time, otherwise the soliton declines away [14]. To compare the newly results with earlier studies, we have selected Maxwellian initial condition

$$z(x, 0) = A \exp\left(-x^2\right) \qquad (28)$$

along the region $-45 \leq x \leq 45$. By using Maxwellian initial condition $I = A\sqrt{\pi}$ obtained so that if $A > \sqrt{\pi} = 1.7725$ use a soliton will appear.

The characteristics of solutions for value of $A = 1$ and $A = 1.78$ time running up from $t = 0$ to $t = 6$ are given in Figure 3. As it is seen from Figure 3, the approximate solution of $|z|$ decay as time increases for value of $A = 1$ unless for the value of $A = 1.78$ soliton's amplitude, shape and speed are preserved. At the same time the position of soliton do not change for both values of $A = 1$ and $A = 1.78$. Numerical results for $A = 1$ with values of $\Delta t = 0.01$ and $N = 611$ are calculated,

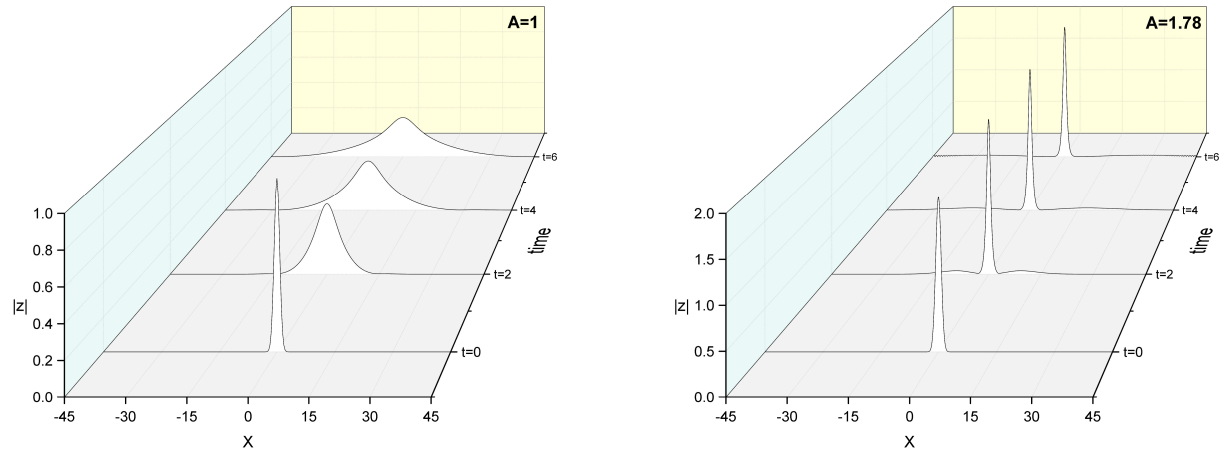

Figure 3. The standing soliton: $A = 1, A = 1.78$.

Table 7. Invariants and relative change of invariants of formation of standing soliton: A=1.

	FDM-DQM			
t	I_1	I_2	$\widehat{I_1}$	$\widehat{I_2}$
0.0	1.25331	0.36711	-	-
0.5	1.25331	0.36712	-8.0×10^{-7}	9.5×10^{-6}
1.0	1.25331	0.36712	-3.9×10^{-6}	1.9×10^{-5}
1.5	1.25331	0.36712	-4.8×10^{-6}	2.6×10^{-5}
2.0	1.25331	0.36712	-6.4×10^{-6}	3.1×10^{-5}
2.5	1.25331	0.36712	-4.8×10^{-6}	2.9×10^{-5}
3.0	1.25330	0.36712	-8.8×10^{-6}	1.4×10^{-5}
3.5	1.25330	0.36711	-1.0×10^{-5}	-3.8×10^{-6}
4.0	1.25330	0.36713	-7.9×10^{-6}	4.0×10^{-5}
4.5	1.25330	0.36714	-1.2×10^{-5}	6.6×10^{-5}
5.0	1.25330	0.36714	-1.4×10^{-5}	7.7×10^{-5}
5.5	1.25330	0.36715	-1.4×10^{-5}	8.7×10^{-5}
6.0	1.25329	0.36713	-1.9×10^{-5}	5.8×10^{-5}

Table 8. Two lowest invariants of the standing soliton: A=1.78

	FDM-DQM		Tay.Coll. [21]		Cub. Coll. [15]		Quad.Gal. [19]		Quin. Coll. [22]	
t	I_1	I_2	I_1	I_2	I_1	I_2	I_1	I_2	I_1	I_2
0.0	3.97100	-4.92558	3.971000	-4.925617	3.97100	-4.9387	3.97100	-4.90562	3.97100	-4.92562
0.5	3.97105	-4.92610	3.965336	-4.911705						
1.0	3.97098	-4.92566	3.967435	-4.925296			3.97099	-4.88626	3.97100	-4.93240
1.5	3.97096	-4.92554	3.967038	-4.910169						
2.0	3.97093	-4.92539	3.966703	-4.908872			3.97099	-4.88421	3.97100	-4.93377
2.5	3.97088	-4.92514	3.967008	-4.910052						
3.0	3.97085	-4.92496	3.967031	-4.910143	3.97095	-4.9387	3.97099	-4.88477	3.97100	-4.93326
3.5	3.97084	-4.92469	3.966839	-4.909396	3.97095	-4.9389				
4.0	3.97080	-4.92446	3.966927	-4.909737	3.97095	-4.9387	3.97099	-4.88472	3.97100	-4.93335
4.5	3.97076	-4.92420	3.967020	-4.910098	3.97095	-4.9386				
5.0	3.97074	-4.92385	3.966900	-4.909633	3.97093	-4.9390	3.97099	-4.88456	3.97100	-4.93346
5.5	3.97072	-4.92335	3.966890	-4.909550	3.97093	-4.9400				
6.0	3.97070	-4.92271	3.966994	-4.909682	3.97094	-4.9416	3.97099	-4.88157	3.97100	-4.93298

and reported in Table 7. As it is seen undoubtedly from Table 7 that FDM-DQM results in two invariants I_1 and I_2 which are nearly constant and acceptable good. Numerical results for $A = 1.78$ with values of $\Delta t = 0.005$ and $N = 721$ are computed and illustrated in Table 8. One can easily see from Table 8 that FDM-DQM produces two invariants I_1 and I_2 which are nearly constant and acceptable good.

4.4. The mobile soliton

As the fourth and the last test problem, the mobile soliton is used with the following initial condition

$$z(x,0) = A\exp\left(-x^2 + 2ix\right) \tag{29}$$

along the domain $-45 \leq x \leq 45$.

The characteristics of solutions for values of $A = 1$ and $A = 1.78$ from time $t = 0$ to $t = 6$ are illustrated in Figure 4. As one can see from Figure 4, the approximate solution of $|z|$ decay as time increases for value of $A = 1$ unless the value of $A = 1.78$ soliton's amplitude, shape and speed are preserved. Numerical results for $A = 1$ with values of $\Delta t = 0.01$ and $N = 581$ are computed and illustrated in Table 9. As one can see obviously from Table 9, FDM-DQM results in two invariants I_1 and I_2 which are almost constant and acceptable good. Numerical results for $A = 1.78$ with values of $\Delta t = 0.005$ and $N = 691$ are computed and tabulated in Table 10. As one can see obviously from Table 10, FDM-DQM yields the two invariants I_1 and I_2 which are nearly constant and acceptable good.

5. Conclusion

In this manuscript, we have applied quartic B-spline based FDM-DQM to obtain the numerical solution of NLS equation. During the solution procedure, to be able to calculate the complex value of function z, we have converted it into the coupled real value functions. For obtaining the second order derivative approximation, differential quadrature method based on fourth order quartic B-spline is used. After that, four famous trial problems have been solved. Simulation of the all of the test problems namely single soliton, double solitons, the standing soliton and mobile soliton given in the Figure 1−Figure 4. As it seen at the Figure 1−Figure 4 that properties of the solitons observed clearly. The efficiency of the method has been tested by calculating the error norms L_2 and L_∞, and two lowest invariants I_1 and I_2 and their relative changes given in the Table 2−Table 10. As one can see from the comparison of the the error norms of the newly method and earlier studies, FDM-DQM results are obviously the best one except for the single soliton at time $t = 2.5$ obtained by Gaussian radial basis collocation method [20]. The already found results clearly indicate that FDM-DQM can also be utilized to obtain numerical results of the NLS equation with high efficiency.

References

[1] Demir, H., & Şahin, S. (2016). Numerical investigation of a steady flow of an incompressible fluid in a lid driven cavity. *Turkish Journal of Mathematics and Computer Science*, 1, 14-23.

[2] Yokus, A., Baskonus, H.M., Sulaiman, T.A., & Bulut, H. (2018). Numerical simulation and solutions of the two-component second order KdV evolutionary system. *Numerical Methods for Partial Differential Equations*, 34, 211-227.

[3] Demir, H., & Süngü, İ. Ç. (2009). Numerical solution of a class of nonlinear Emden-Fowler equations by using differential transform method. *Cankaya University Journal Science and Engineering*, 12, 75-81.

[4] Demir, H., & Baltürk, Y. (2017). On numerical solution of fractional order boundary value problem with shooting method. *ITM Web of Conferences*, 13, 01032.

[5] Demir, H., & Ertürk, V.S. (2001). A numerical study of wall driven flow of a viscoelastic fluid in rectangular cavities. *Indian Journal of Pure and Applied Mathematics*, 32(10), 1581-1590.

[6] Yokus, A., Sulaiman, T.A., Baskonus, H.M., & Atmaca, S.P. (2018). On the exact and numerical solutions to a nonlinear model arising in mathematical biology. *ITM Web of Conferences*, 22, 01061.

[7] Karpman, V.I., & Krushkal, E.M. (1969). Modulated waves in non-linear dispersive media. *Soviet Physics—JETP*, 28, 277.

[8] Scott, A.C., Chu, F.Y.F., & Mclaughlin, D.W. (1973). The soliton: A new concept in applied science, *Proceedings of the IEEE*, 61(10),1443-1483.

[9] Zakharov, V.E., & Shabat, A.B. (1972). Exact theory of two dimensional self focusing and one dimensional self waves in non-linear media. *Soviet Journal of Experimental and Theoretical Physics*, 34,62.

[10] Delfour, M., Fortin, M., & Payre, G. (1981). Finite-difference solutions of a non-linear Schrödinger equation. Journal of Computational Physics, 44, 277-288.

[11] Thab, T.R., & Ablowitz, M.J. (1984). Analytical and numerical aspects of certain nonlinear evolution equations. II, Numerical, nonlinear Schrödinger equations. *Journal of Computational Physics*, 55, 203-230.

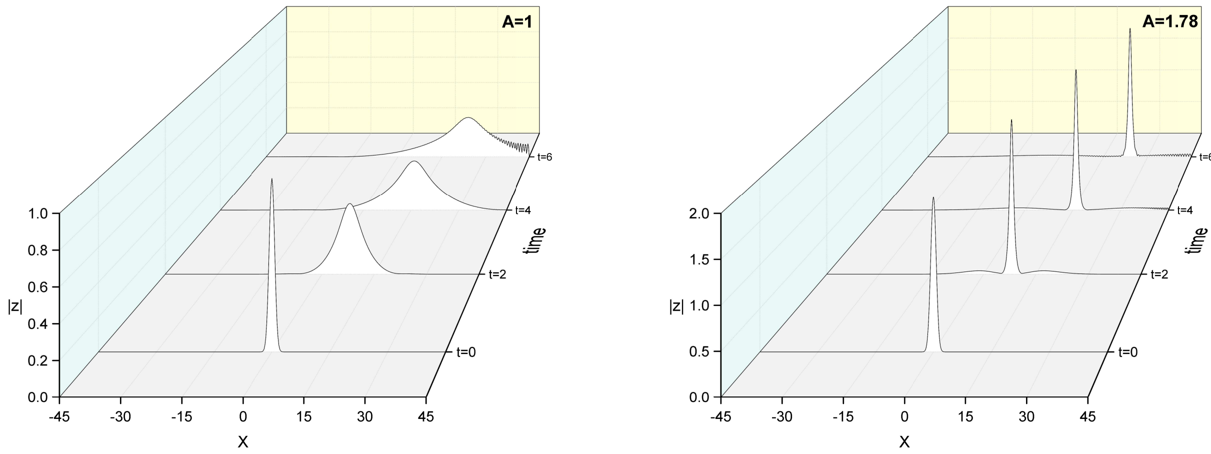

Figure 4. The mobile soliton: $A = 1, A = 1.78$.

Table 9. Invariants of mobile soliton:A=1.

	FDM-DQM			
t	I_1	I_2	$\widehat{I_1}$	$\widehat{I_2}$
0	1.25331	5.38148	-	-
1	1.25324	5.37853	-5.9×10^{-5}	-5.5×10^{-4}
2	1.25324	5.37795	-6.1×10^{-5}	-6.6×10^{-4}
3	1.25323	5.37768	-6.5×10^{-5}	-7.1×10^{-4}
4	1.25324	5.37761	-6.2×10^{-5}	-7.2×10^{-4}
5	1.25325	5.37758	-5.5×10^{-5}	-7.3×10^{-4}
6	1.25328	5.37752	-2.9×10^{-5}	-7.4×10^{-4}

Table 10. Invariants of mobile soliton:A=1.78

	FDM-DQM		Quin. Coll. [22]		Cub. Coll. [15]		Quad.Gal. [19]		Tay.Coll. [21]	
t	I_1	I_2	I_1	I_2	I_1	I_2	I_1	I_2	I_1	I_2
0	3.97100	10.96012	3.97100	10.95837	3.97100	10.9583	-	-	-	-
1	3.97111	10.96130	3.97100	10.97104	3.97101	10.2915	3.97096	11.34136	3.96377	10.93552
2	3.97114	10.96184	3.97100	10.97294			3.97095	11.36011	3.96199	10.93271
3	3.97114	10.96234	3.97100	10.97289			3.97095	11.35076	3.96292	10.93364
4	3.97114	10.96272	3.97100	10.97336	3.97100	8.50	3.97095	11.35546	3.96250	10.93377
5	3.97112	10.96289	3.97100	10.97374	3.97101	8.05	3.97095	11.35412	3.96255	10.93385
6	3.97107	10.96299	3.97100	10.97592			3.97123	11.38259	3.96276	10.93627

[12] Argyris, J., & Haase, M. (1987). An engineer's guide to soliton phenomena: Application of the finite element method. *Computer Methods in Applied Mechanics and Engineering*, 61, 71-122.

[13] Twizell, E.H., Bratsos, A.G., & Newby, J.C. (1997). A finite-difference method for solving the cubic Schrödinger equation. *Mathematics and Computers in Simulation*, 43,67-75.

[14] Gardner, L.R.T., Gardner, G.A., Zaki, S.I., & El Sharawi, Z.(1993). A leapfrog algorithm and stability studies for the non-linear Schrödinger equation. *Arabian Journal for Science and Engineering*, 18(1), 23-32.

[15] Gardner, L.R.T., Gardner, G.A., Zaki, S.I., & El Sharawi, Z.(1993). B-spline finite element studies of the non-linear Schrödinger equation. *Computer Methods in Applied Mechanics and Engineering*, 108, 303-318.

[16] Herbst, B.M., Morris, J. Ll. & Mitchell, A.R. (1985). Numerical experience with the nonlinear Schrödinger equation. *Journal of Computational Physics*, 60, 282-305.

[17] Robinson, M.P., & Fairweather, G. (1994). Orthogonal spline collocation methods for Schrödinger-type equation in one space variable. *Numerische Mathematik*, 68(3), 303-318.

[18] Robinson, M.P. (1997). The solution of nonlinear Schrödinger equations using orthogonal spline collacation. *Computers & Mathematics with Applications*, 33(7), 39-57.

[19] Dağ, I. (1999). A quadratic b-spline finite element method for solving the nonlinear Schrödinger equation. *Computer Methods in Applied Mechanics and Engineering*, 174, 247-258.

[20] Dereli, Y., Irk, D., & Dag, I. (2009). Soliton solutions for NLS equation using radial basis functions. *Chaos, Solitons and Fractals*, 42, 1227-1233.

[21] Aksoy, A.M., Irk, D., & Dag, I. (2012). Taylor collocation method for the numerical solution of the nonlinear Schrödinger equation using quintic b-spline basis. *Physics of Wave Phenomena*, 20(1), 67-79.

[22] Saka, B. (2012). A quintic B-spline finite-element method for solving the nonlinear Schrödinger equation. *Physics of Wave Phenomena*, 20(2), 107-117.

[23] Shu, C. (2000). *Differential quadrature and its application in engineering*. Springer-Verlag, London.

[24] Bellman, R., Kashef, B.G., & Casti, J. (1972). Differential quadrature: a tecnique for the rapid solution of nonlinear differential equations. *Journal of Computational Physics*, 10, 40-52.

[25] Zhong, H. (2004). Spline-based differential quadrature for fourth order equations and its application to Kirchhoff plates. *Applied Mathematical Modelling,* 28, 353-366.

[26] Shu, C., & Xue, H. (1997). Explicit computation of weighting coefficients in the harmonic differential quadrature. *Journal of Sound and Vibration,* 204(3), 549-555.

[27] Cheng, J., Wang, B., & Du, S. (2005). A theoretical analysis of piezoelectric/composite laminate with larger-amplitude deflection effect, Part II: hermite differential quadrature method and application. *International Journal of Solids and Structures*, 42, 6181-6201.

[28] Shu, C. & Wu, Y.L. (2007). Integrated radial basis functions-based differential quadrature method and its performance. *International Journal for Numerical Methods in Fluids*, 53, 969-984.

[29] Korkmaz, A., Aksoy, A.M., & Dağ, I. (2011). Quartic b-spline differential quadrature method. *International Journal of Nonlinear Science*, 11(4), 403-411.

[30] Başhan, A., Yağmurlu, N.M., Uçar, Y., & Esen, A. (2018). A new perspective for the numerical solutions of the cmKdV equation via modified cubic B-spline differential quadrature method. International *Journal of Modern Physics C*, 29(06), 1850043.

[31] Karakoc, S.B.G., Başhan A., & Geyikli, T. (2014).Two different methods for numerical solution of the modified burgers' equation. *The Scientific World Journal*,2014, Article ID 780269, 13 pages, http://dx.doi.org/10.1155/2014/780269

[32] Başhan, A., Karakoç, S.B.G., & Geyikli, T. (2015). Approximation of the KdVB equation by the quintic B-spline differential quadrature method. *Kuwait Journal of Science*, 42(2), 67-92.

[33] Başhan, A., Karakoç, S.B.G., & Geyikli, T. (2015). B-spline differential quadrature method for the modified burgers' equation. *Çankaya University Journal of Science and Engineering*, 12(1), 001-013.

[34] Başhan, A., Uçar, Y., Yağmurlu, N.M., & Esen, A. (2016). Numerical solution of the complex modified Korteweg-de Vries equation by DQM. *Journal of Physics: Conference Series* 766, 012028 doi:10.1088/1742-6596/766/1/012028

[35] Başhan, A., (2018). An effective application of differential quadrature method based on modified cubic B-splines to numerical solutions of KdV equation. *Turkish Journal of Mathematics*, 42, 373-394. DOI: 10.3906/mat-1609-69.

[36] Rubin, S.G., & Graves, R.A. (1975). A cubic spline approximation for problems in fluid mechanics. NASA technical report, NASA TR R-436.

[37] Prenter, P.M. (1975). *Splines and Variational Methods*. John Wiley, New York.

Ali Başhan *received his undergraduate degree in mathematics education from the Marmara University in 2003. He has completed his M.Sc. at Fırat University and Ph.D. degree at Inonu University in applied mathematics. He is currently studying about the numerical solutions of the partial differential equations. His research interests include finite difference methods and differential quadrature methods.*